Thermal and Well Flow Performance of Closed-Loop Geothermal in the Wattenberg Area

Preprint

Dayo Akindipe, Abra Gold, Geoffrey Kiptoo Mibei, Adam Ketchum, and Koenraad Beckers

National Renewable Energy Laboratory

Presented at the 2024 Geothermal Rising Conference
Waikoloa, Hawai'i
October 27-30, 2024

NREL is a national laboratory of the U.S. Department of Energy
Office of Energy Efficiency & Renewable Energy
Operated by the Alliance for Sustainable Energy, LLC

This report is available at no cost from the National Renewable Energy Laboratory (NREL) at www.nrel.gov/publications.

Contract No. DE-AC36-08GO28308

Conference Paper
NREL/CP- 5700-90798
October 2024

Thermal and Well Flow Performance of Closed-Loop Geothermal in the Wattenberg Area

Preprint

Dayo Akindipe, Abra Gold, Geoffrey Kiptoo Mibei, Adam Ketchum, and Koenraad Beckers

National Renewable Energy Laboratory

Suggested Citation
Akindipe, Dayo, Abra Gold, Geoffrey Kiptoo Mibei, Adam Ketchum, and Koenraad Beckers. 2024. *Thermal and Well Flow Performance of Closed-Loop Geothermal in the Wattenberg Area*. Golden, CO: National Renewable Energy Laboratory. NREL/TP-5700-90798. https://www.nrel.gov/docs/fy25osti/90798.pdf.

NREL is a national laboratory of the U.S. Department of Energy
Office of Energy Efficiency & Renewable Energy
Operated by the Alliance for Sustainable Energy, LLC

This report is available at no cost from the National Renewable Energy Laboratory (NREL) at www.nrel.gov/publications.

Contract No. DE-AC36-08GO28308

Conference Paper
NREL/CP-5700-90798
October 2024

National Renewable Energy Laboratory
15013 Denver West Parkway
Golden, CO 80401
303-275-3000 • www.nrel.gov

NOTICE

This work was authored by the National Renewable Energy Laboratory, operated by Alliance for Sustainable Energy, LLC, for the U.S. Department of Energy (DOE) under Contract No. DE-AC36-08GO28308. Funding provided by the U.S. Department of Energy Geothermal Technologies Office. The views expressed herein do not necessarily represent the views of the DOE or the U.S. Government.

Cover Photos by Dennis Schroeder: (clockwise, left to right) NREL 51934, NREL 45897, NREL 42160, NREL 45891, NREL 48097, NREL 46526.

Thermal and Well Flow Performance of Closed-Loop Geothermal in the Wattenberg Area

Dayo Akindipe, Abra Gold, Geoffrey Kiptoo Mibei, Adam Ketchum and Koenraad Beckers

National Renewable Energy Laboratory

Keywords

Closed-loop geothermal, slender body theory, Wattenberg anomaly, techno-economic analysis

ABSTRACT

Closed-loop geothermal systems provide an alternative to resource-constrained hydrothermal systems and stimulation-intensive enhanced geothermal systems. In this work, we apply the slender-body theory (SBT) model, to simulate the well flow and heat transfer performance of U-loop well designs in the Wattenberg area of the Denver-Julesburg Basin. Three U-loop well patterns are investigated, including a single-, double-, and multi-lateral design. The subsurface within the area of interest is characterized by deep, hot (> 200°C) igneous/metamorphic basement rock underlying multiple sedimentary formations. The lateral section(s) of the U-loop lie(s) within a target depth of 6 km, where temperatures are estimated to approach 300°C. As a base case, conduction-only heat transfer is investigated through simulations with the SBT model within U-loops with open-hole laterals that exchange heat directly with the hot, dry rock using water as a working fluid. The utilization of supercritical CO_2 as a heat transfer fluid is also considered. For each scenario, the system performance in terms of annual heat production and temperature profile over a 20-year project lifetime are assessed. Also, the levelized costs of heat and electricity (LCOH and LCOE) are determined using a top-down techno-economic analysis model. The results show that the performance- and cost-optimized U-loop design is one having an injection-production well spacing of 1,000 meters with ten 50-meter-spaced laterals that traverse a subsurface system with a temperature gradient of 60°C/km. By injecting 20°C-water at a rate of 60 kg/s through this loop, an average heat production of 19 MW_{th} (i.e., 2.2 MW_e net plant output) can be achieved, resulting in an LCOE and LCOH of \$136/MWh_e and \$1.53/GJ, respectively, over a 20-year project life.

1. Introduction

A first-of-a-kind geothermal drilling project in Colorado, titled the Geothermal Limitless Approach to Drilling Efficiencies (GLADE), has been funded by the Geothermal Technologies Office (GTO) of the U.S. Department of Energy (DOE). The project aims to significantly improve drilling rates by combining proven and novel drilling technology and analytics to safely drill twin high-temperature wells in the Wattenberg area of the Denver-Julesburg (D-J or Denver) Basin (Figure 1). The D-J Basin is a structural basin with a large asymmetric syncline comprising Paleozoic, Mesozoic, and Cenozoic sedimentary rock layers underlain by a Precambrian basement

with igneous and metamorphic lithology (Curtis, 1988). The local vertical depth to the basement is expected to be in the range ~3,000 to ~3,800 m (Porro et al., 2012). A representative cross section along the line A-A' of Figure 1 is shown in Figure 2. The sedimentary layers are dominated by subaerial deposits, with minimal carbonates (Abbott & Noe, 2004). Oil and gas production occurs from several formations in the basin, including the Pierre shale, lower Cretaceous formations, and the Lyons sandstone (Nelson & Santus, 2011; Crowell et al., 2012). Using aeromagnetic surveys and cross-correlation with exposed bedrocks in the Front Range, Sims et al. (2001) interpreted bedrocks through Colorado and established that, for the study area, the expected basement lithology consists of either Paleoproterozoic gneiss or Paleoproterozoic granite (Sims et al., 2001).

The Greater Wattenberg area is associated with a thermal anomaly characterized by higher geothermal gradients than the surrounding area (Weimer, 1996). The youngest rocks observed are predominantly sedimentary, devoid of indications of recent volcanism. The heat source for the observed anomalous geothermal gradients is not well understood, because the deepest wells in the Denver Basin penetrate only to about 2,700 m in depth (Higley & Cox, 2007). The complex structure in the deep basin (reverse faults associated with brittle deformation and basin buckling), underlain by conductive minerals in the basement rock are factors that could concentrate heat in the region. This model for anomalous heat flow in a sedimentary basin is consistent with geothermal "play types" that develop in the foreland basin of a conduction-dominated orogenic belts (Moeck, 2014; Davalos-Elizondo et al., 2023). Thermal replenishment has been hypothesized to be supported by either deep-seated magmatic intrusions, an upflow zone of a deep hot water system facilitated by faults, or a deep conductive zone created by mineralization of highly conductive minerals associated with the Colorado Mineral Belt (Eaton, 2023). Geological data from planned deep wells may help shed light on heat and fluid sources in the Wattenberg area.

Using bottom hole measurement data from 6,181 oil and gas wells drilled in the area, Lacazette et al. (2024) developed isotherms around the major hot spot in the Wattenberg area. Their map revealed a thermal gradient between 40°C/km and 60°C/km in the hot spot (Lacazette et al., 2024). The target vertical depth of the proposed twin wells is on the order of 6.1 km, significantly surpassing the Phanerozoic sedimentary layers and into the Precambrian basement. There, it is anticipated that temperatures at the target depth could be between 240°C and 360°C. At these temperatures the thermal energy from the subsurface could be primarily harnessed for geothermal power with next-generation geothermal technologies, including closed-loop geothermal (CLG) and enhanced geothermal systems (EGS). With a CLG/EGS development in a conduction-only reservoir, heat extraction typically proceeds faster than natural replenishment rates, resulting in a long-term decline of reservoir and production temperature (Fox et al., 2013). Heat transfer in low-thermal conductivity basement rocks, such as those in the Wattenberg area, is presumed to proceed at slow rates requiring significant time for thermal replenishment in the target reservoir after depletion.

In this work, we apply the slender-body theory (SBT) model to simulate the well flow and heat transfer performance of possible closed-loop (U-loop) well designs drilled in the Wattenberg area of the Denver Basin. Three U-loop designs are investigated, including a (a) single-lateral, (b) double-lateral, and (c) multi-lateral design. We have also compared the performance of both water and carbon dioxide (CO_2) as working fluids for the closed-loop heat transfer process. Finally, we

determine and compare the cost of each design option to determine the most feasible design for electricity generation and heating applications.

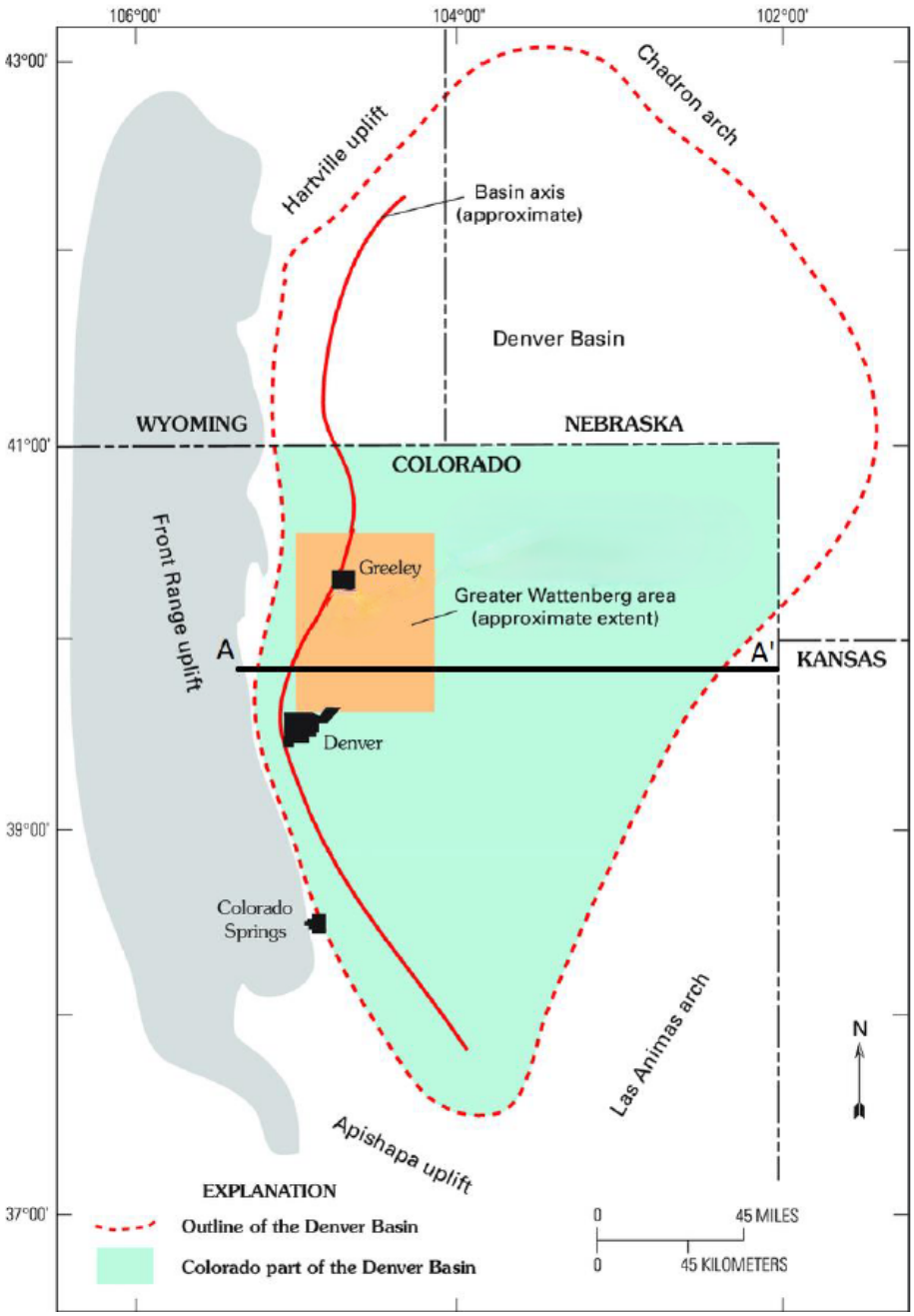

Figure 1: Greater Wattenberg area (orange rectangle) in the Denver Basin (approximate extent shown with red dashed line). The A-A' cross section is shown in Figure 2. The figure was modified from Roberts (2007).

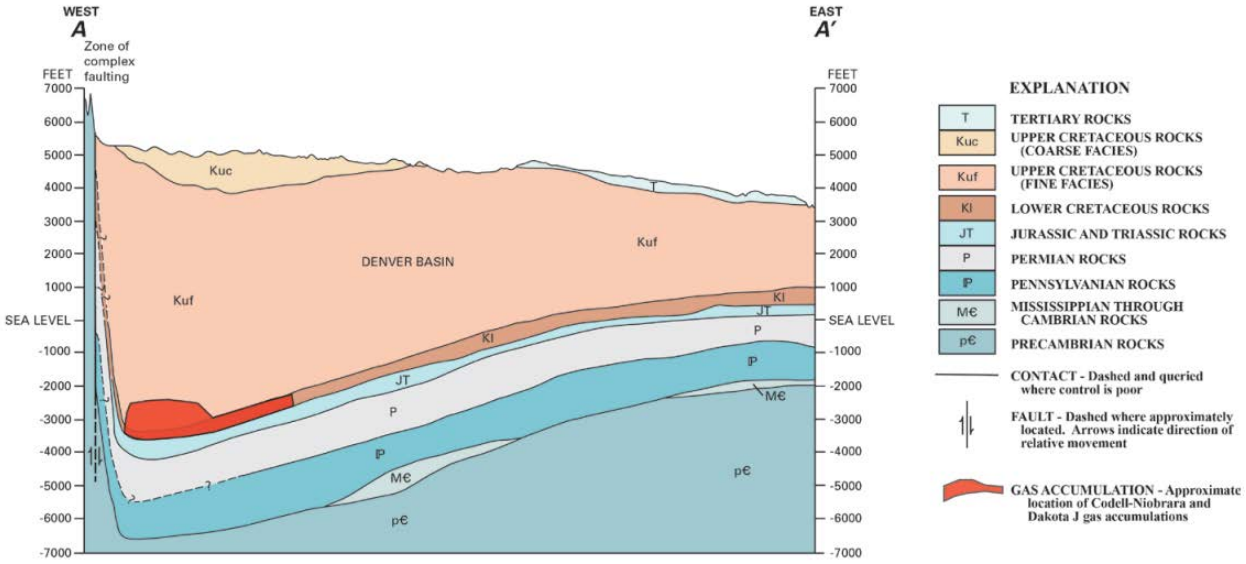

Figure 2: Representative cross section for the Denver Basin along the line A-A' in Figure 1. The Denver Basin is a large asymmetric syncline with a deepest point about 3,900 m below surface. The figure is from Nelson and Santus (2011).

2. Slender Body Theory (SBT) Modeling for Closed-Loop Well Designs

The SBT model is a MATLAB-based tool used for wellbore simulation that effectively models heat exchange, fluid profiles, and pressure profiles for closed-loop geothermal systems without high computational demand (Beckers & Johnston, 2022). By asymptotically matching a three-dimensional infinite cylinder to a one-dimensional finite line source, the model solves for temperature and pressure at each tubing element along the wellbore that is undergoing conductive heat transfer with the rock. Further information about the theory and the model implementation is found in (Beckers et al., 2015; Beckers & Johnston, 2022). The SBT is applicable to this study because the vertical distance covered by the loop is so large that the vertical and lateral geometry can be approximated as a slender, one-dimensional track. Therefore, we have applied this model to simulate the effects of altering different wellbore geometric parameters, reservoir fluid properties, and material and flow conditions in a closed-loop geothermal system to determine an optimal design from a standard base case within a conductive subsurface domain.

2.1 Closed-Loop Wellbore Geometry

We have designed twin wells based on a synthetic wellbore trajectory. The system envisioned consists of two parallel wells with a total vertical depth of 6.1 km and connected at the bottom by one or multiple laterals, depending on the investigated scenario. It is important to state that the designed well patterns are not representative of the actual well plan for the GLADE project, which is still under development.

2.1.1 Base Case

First, we implemented a base case scenario in the SBT tool, with the geometry shown in Figure 3. Both injection and productions wells have a straight vertical section down to a depth of 3,100 m,

followed by an inclined section with an angle of 12 degrees down to a vertical depth of about 6.1 km. The base case geometric properties are as described below:

- Two laterals were simulated in the Y-dimension between the production and injection wells at depth.
- Injection and production wells reached a vertical depth of 6.1 km.
- The vertical injection and production wellbore radius was 0.108 m (radius = 4.25 in; diameter = 8.5 in) and was uniform in both wells.
- The lateral wellbore radius was 0.108 m (radius = 4.25 in; diameter = 8.5 in).
- The pipe internal wall roughness was 1×10^{-6} m.
- The lateral length horizontally connecting the injection and production wells was 100 m in the Y-dimension.
- The distance between laterals was 25 m in the X-dimension.

In this and other simulation cases, all wellbores (injection, production, and laterals) along the heat exchanger path were assumed to be open hole with a negligible rock permeability at the well-formation interface. Conduction-only heat transfer between the rock and fluid was simulated, and all simulations were run on a basis of a 20-year operational lifetime. The well designs do not account for wellbore curvature; consequently, laterals are 90 degrees from the vertical direction. Going from 90 degrees to actual curvature would only slightly change total heat exchanger length (and heat transfer area). Therefore, having no curvature is expected to have negligible effect on heat extraction.

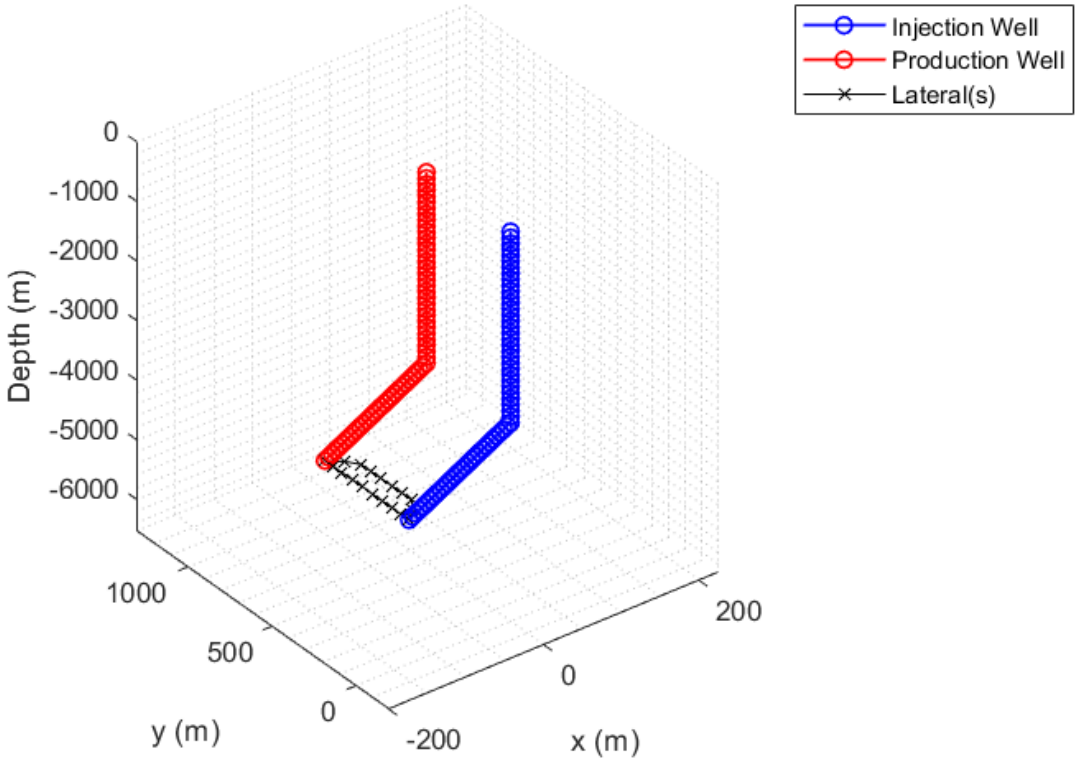

Figure 3: Well geometry schematic for the base case scenario showing the well track notated by colored circles as described in the legend on the right. Lateral length in the Y-dimension has been exaggerated to 500 m for visualization purposes (the original base case lateral length in the Y-dimension is 100 m).

2.1.2 Other Simulation Scenarios

Beyond the base case, we ran multiple simulation scenarios by varying the input parameters relating to the (a) well geometry, (b) flow boundary conditions, and (c) rock and fluid materials to determine the effect of parameter variability on the heat production from the closed-loop system. Table 1 shows the 15 scenarios and the input parameters that were varied in each simulation.

Table 1: The 15 simulation scenarios that were investigated in this work.

Simulation Scenarios	Number of laterals	Lateral spacing (X-direction), m	Well spacing (Y-direction), m	Injection rate, kg/s	Injection temp., °C	Thermal Gradient, °C /km	Rock type	Working fluid
Scenario A (Base case)	2	25	100	40	20	50	Granite	Water
Scenario B	1	25	100	40	20	50	Granite	Water
Scenario C	10	25	100	40	20	50	Granite	Water
Scenario D	2	10	100	40	20	50	Granite	Water
Scenario E	2	50	100	40	20	50	Granite	Water
Scenario F	2	25	500	40	20	50	Granite	Water
Scenario G	2	25	1000	40	20	50	Granite	Water
Scenario H	2	25	100	20	20	50	Granite	Water
Scenario I	2	25	100	60	20	50	Granite	Water
Scenario J	2	25	100	40	40	50	Granite	Water
Scenario K	2	25	100	40	60	50	Granite	Water
Scenario L	2	25	100	40	20	40	Granite	Water
Scenario M	2	25	100	40	20	60	Granite	Water
Scenario N	2	25	100	40	20	50	Gneiss	Water
Scenario O	2	25	100	40	20	50	Granite	CO_2

2.2 Fluid and Rock Thermophysical Properties

We simulated water and CO_2 as working fluids. Variable fluid properties were employed, allowing pressure and temperature to affect the density, specific heat capacity, thermal conductivity, and dynamic viscosity of both fluids. Granite and gneiss (Table 2) were used in two simulated cases. It is noteworthy that the subsurface geology in the study area is not homogeneous. There is a high uncertainty in the lithology of the basement rock in the Wattenberg area due to the unavailability of well data at the target depth. To account for the effect of the overburden sedimentary lithology, we have used the same depth-scaled averages for the rock properties and considered only one representative lithology (i.e., granite or gneiss) for the reservoir rock.

Table 2: Thermophysical properties of the two rock types studied in this work.

Lithology	Density, kgm^{-3}	Heat capacity, $Jkg^{-1}K^{-1}$	Thermal Conductivity, $Wm^{-1}K^{-1}$
Gneiss	2,570	1,080	2.9
Granite	2,540	1,185	3.1

3. System Performance

The base case is the control scenario. This case simulated a production and injection well that was 6.1 km deep with a 0.108-m radius. Two laterals were simulated that connected the production and injection wells. These laterals were approximately 100-m long and spaced approximately 25 m apart (Figure 3). Granite was the reservoir rock, and a constant ground surface temperature was selected at 20°C. The results of the base case simulation presented in Table 3 reveal an average production temperature, final temperature, and heat production of 56.1°C, 53.3°C, and 6 MW_{th}, respectively. In the remainder of this section, we probe the effect of well geometry, boundary conditions, and rock and fluid characteristics on the system performance.

Table 3: Output variables of average temperature, final temperature, and heat production for the 15 scenarios after a 20-year simulation.

Simulation Scenarios	Avg. Production Temperature, °C	Final Temperature, °C	Avg. Heat Production, MW_{th}
Scenario A (Base case)	56.1	53.3	6.00
Scenario B	55.4	52.7	5.88
Scenario C	64.7	60.8	7.44
Scenario D	55.4	52.7	5.90
Scenario E	56.3	53.5	6.03
Scenario F	59.7	56.6	6.61
Scenario G	64.3	60.6	7.38
Scenario H	83.0	78.9	5.26
Scenario I	45.3	43.3	6.27
Scenario J	71.2	68.9	5.21
Scenario K	86.4	84.4	4.42
Scenario L	48.9	46.7	4.80
Scenario M	63.3	60.0	7.21
Scenario N	54.0	51.4	5.70
Scenario O	68.2	64.7	4.40

3.1 Effect of U-Loop Geometry

3.1.1 Number of Laterals

The number of laterals in the U-loop varied from one, two (base case), and 10 laterals. All other geometry specifications, boundary conditions, and material properties were as in the base case. The general heat production and output temperature trend is an initial high heat production rate (and temperature) followed by a steep decline within the first few weeks of production towards a steady state. This is typical for closed-loop systems with a single (constant) flow rate. It is apparent that 10 laterals offer an elevated average heat production over 20 years (7.44 MW_{th}) compared to both single and double laterals (5.88 and 6.0 MW_{th}, respectively; Figure 4). Scenario C with 10 laterals also results in an elevated outlet temperature compared to Scenarios A and B.

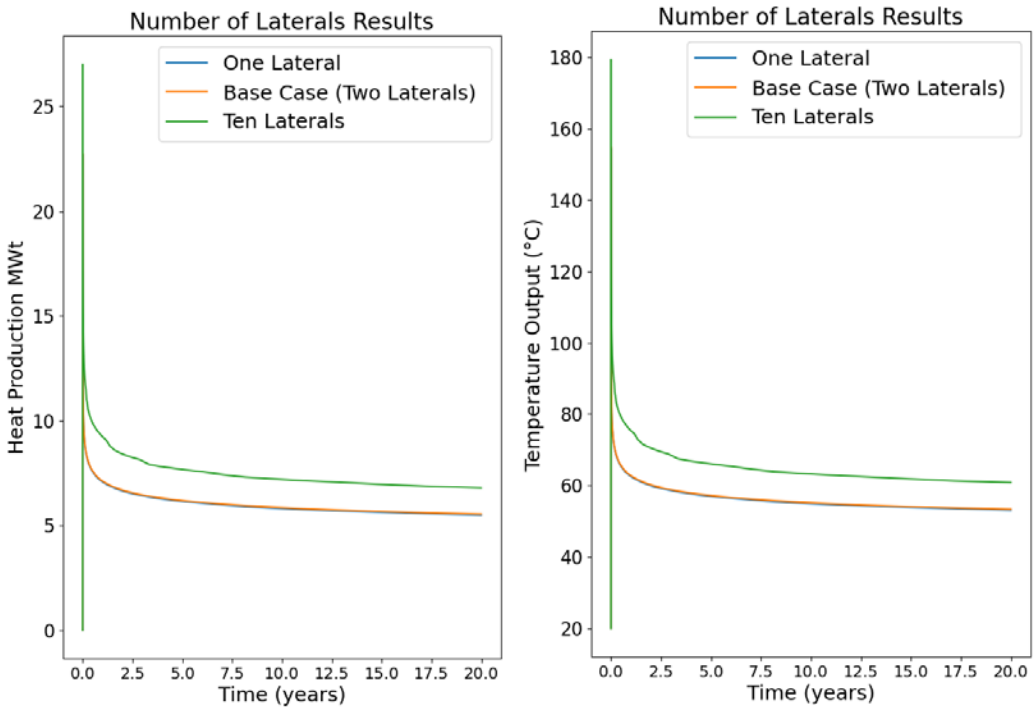

Figure 4: Heat production (MW_{th}) and temperature (°C) output over 20 years for one, two, and 10 laterals. The one- and two-lateral cases overlap due to similar heat production and output temperatures.

3.1.2 Lateral Spacing

Next, 10-m, 25-m (base case), and 50-m lateral spacings in the X-direction were simulated. All other geometry specifications, boundary conditions, and material properties were base case. Simulation results showed that a larger spacing in the X-direction between the laterals increases the outlet temperature by less than 1°C and the average heat production by less than 150 kW (Table 3). This is because, for this well design, thermal interference between laterals is minimal above the 10-m spacing. Therefore, a lateral spacing of 25 m was used as the default to minimize losses due to interference between the laterals.

3.1.3 Well Spacing

The spacing between the injection and production well in the Y-direction was modified from 100 m (base case) to 500 m and 1,000 m in Scenarios F and G, respectively. All other geometry specifications, boundary conditions, and material properties were base case. Extending the well spacing in the Y-direction between the injection and production wells yields an elevated heat production and outlet temperature output (Figure 5).

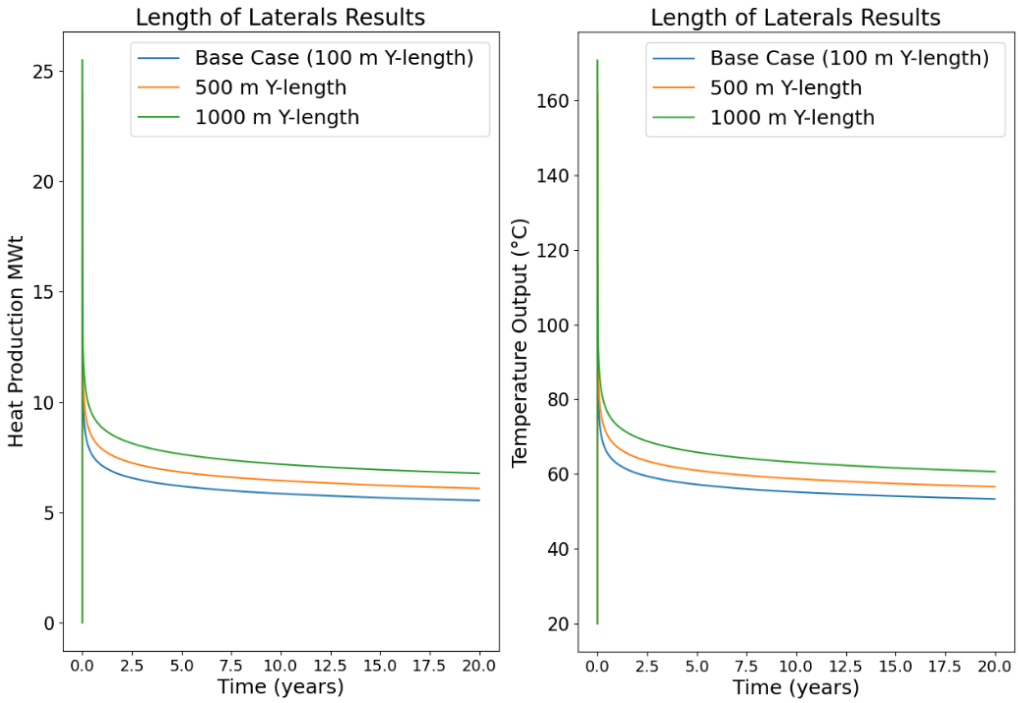

Figure 5: Heat production (MW_{th}) and temperature (°C) output over 20 years for 100-m, 500-m, and 1,000-m length laterals.

3.2 Effect of Boundary Conditions

3.2.1 Injection Rate

The system performance for multiple injection rates of 20 kg/s (Scenario H), 40 kg/s (base case), and 60 kg/s (Scenario I) were compared. All other geometry specifications, boundary conditions, and material properties were the same as the base case. Lower injection rates facilitated lower heat production over time compared to higher injection rate (Figure 6). The opposite trend was observed for outlet temperatures, where lower injection rate had higher output temperature compared to higher injection rates. This is in line with previous observations by Beckers et al. (2022), who reported that decreasing flow rate will decrease heat output, but increase outlet temperature in both co-axial and U-loop systems. This is because the reduction in mass flow is more significant than the slight rise in temperature (due to longer residence time) resulting in a combined effect of lower heat production. This observation suggests that a lower injection rate allows for better outlet temperature control and would benefit applications that need to meet this requirement. For systems that aim to maximize power output, a higher flow rate is necessary.

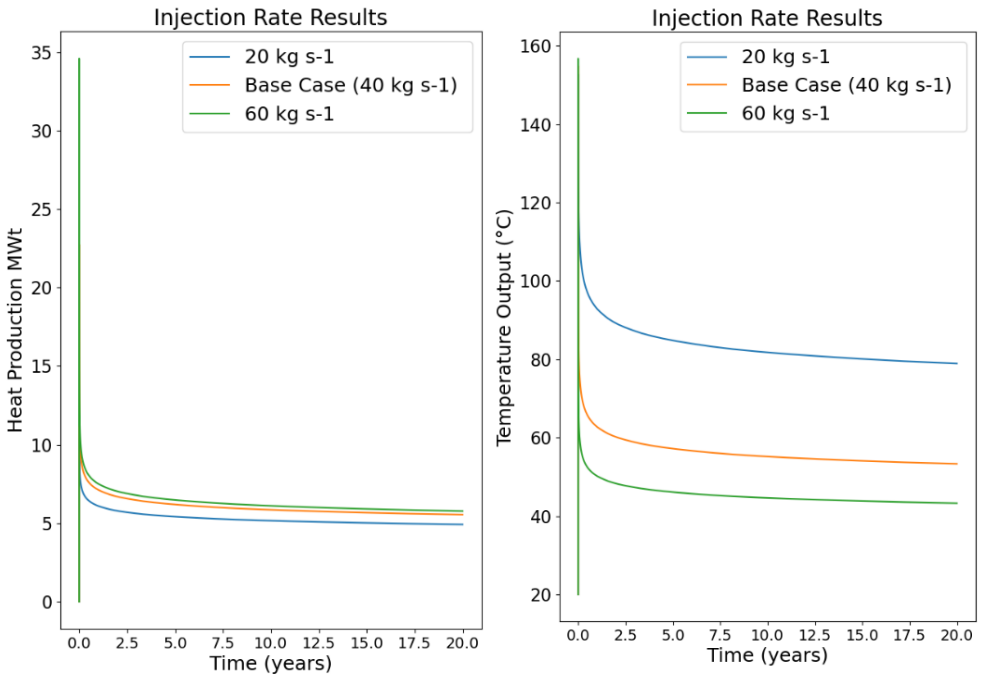

Figure 6: Heat production (MW_{th}) and temperature (°C) output over 20 years for injection rates of 20, 40, and 60 kg/s.

3.2.2 Injection Temperature

To understand the effect of the injection temperature on system performance, we ran simulations for Scenario J (injection temperature = 40°C) and Scenario K (injection temperature = 60°C). The results were compared to the base case with an injection temperature of 20°C. As shown in Figure 7, the higher injection temperatures were characterized by a lower heat production over the project life. The resulting average heat production was 5.21 MW_{th} and 4.42 MW_{th} for Scenario J and Scenario K, respectively. On the other hand, higher injection rates enabled a higher production temperature (Figure 7). Similar to results reported in prior work, increasing injection temperature results in a reduction in the extractable energy (a function of the difference between the reservoir temperature and the injection temperature), which in turn result in a lower heat production (Beckers et al., 2022).

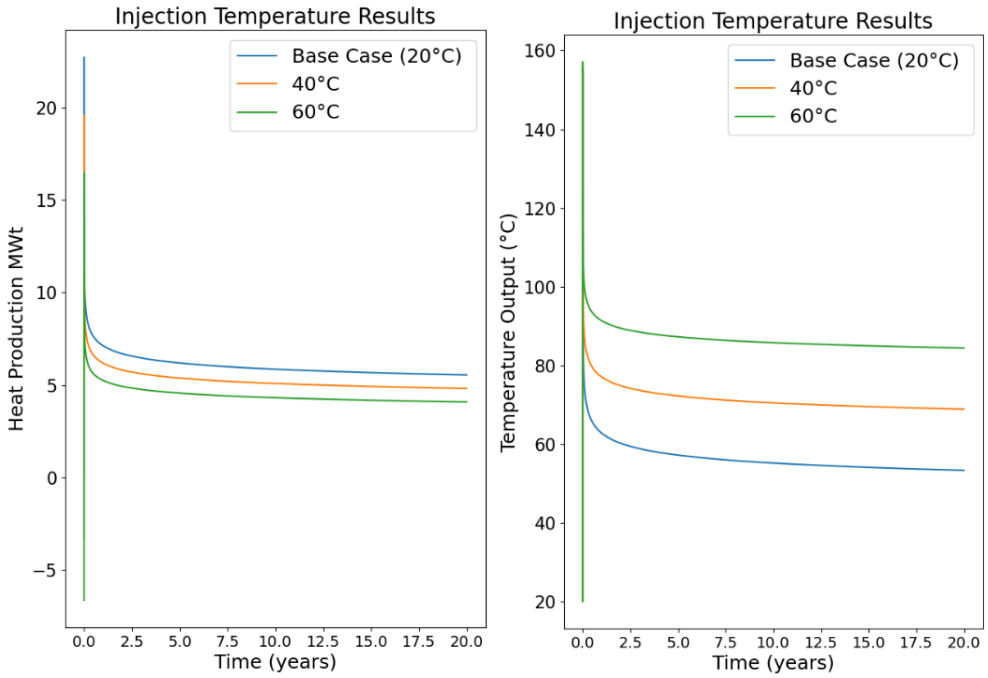

Figure 7: Heat production (MW_{th}) and temperature (°C) output over 20 years for inlet temperatures of 20°C, 40°C, and 60°C.

3.2.3 Geothermal Gradient

Variations of the subsurface geothermal gradient were employed as 40°C/km (Scenario L), 50°C/km (base case), and 60°C/km (Scenario M). All other geometry specifications, boundary conditions, and material properties were base case. Overall, it is apparent that higher heat production and outlet temperature throughout the project life are directly correlated to the magnitude of the geothermal gradient (Figure 8).

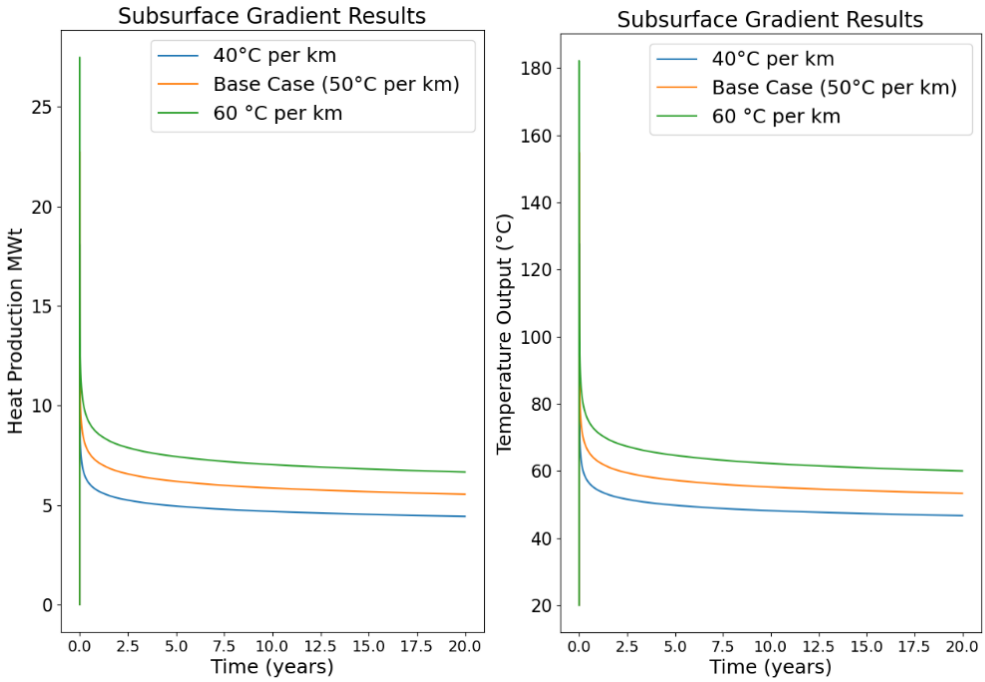

Figure 8: Heat production (MW_{th}) and temperature (°C) output over 20 years for 40°C/km, 50°C/km, and 60°C/km.

3.3 Effect of Rock and Fluid Types

3.3.1 Rock Type

To understand and quantify the uncertainty in the lithology of the basement rock and its effect on thermal performance, we completed simulations for the two end cases, i.e., the base case with granite and Scenario N with gneiss. The results in Table 3 show that a gneiss basement lithology results in lower output temperature and heat production over the project life. This arises from a combination of a higher thermal conductivity and heat capacity for the same volume of granite compared to gneiss.

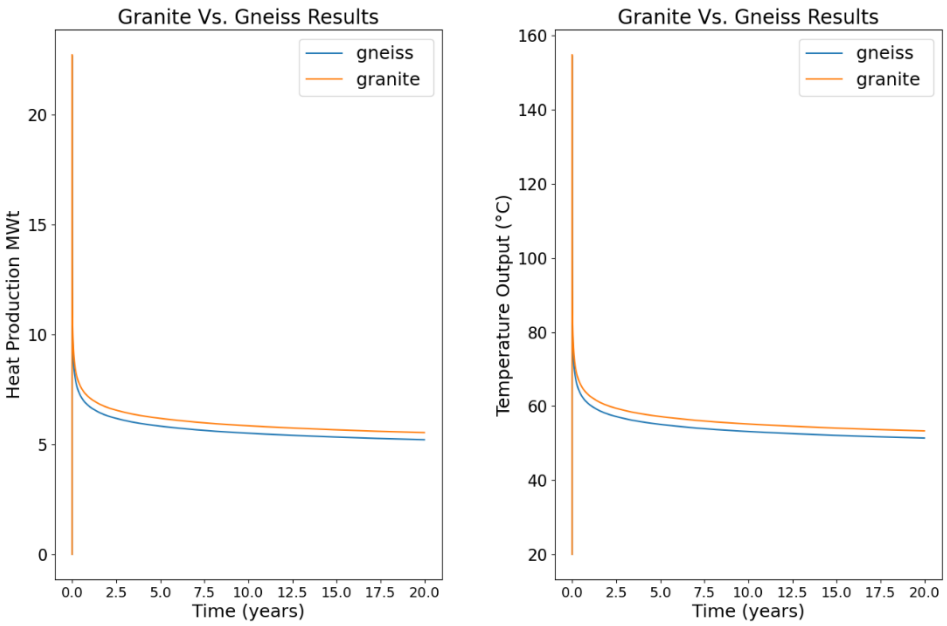

Figure 9: Heat production (MW_{th}) and temperature (°C) output over 20 years for gneiss versus granite.

3.3.2 Working Fluid

The thermal property and composition of the working fluid in a closed-loop system are important factors that influence performance. In this study, water and CO_2 were compared. At a constant injection wellhead pressure of 100 bar, the CO_2 is supercritical within the closed loop system as it traverses the reservoir domain and the production well. As displayed in Figure 10, the average production temperature for a CO_2-based U-loop was elevated compared to water, yet the opposite was evident for average heat production. Water shows an elevated average heat production (6.0 MW_{th}) compared to CO_2 (4.4 MW_{th}). The higher heat production is mainly due to the higher specific heat capacity of water compared to CO_2 (4.2 versus 0.84 J kg^{-1} K^{-1}). However, the higher outlet temperatures for CO_2 arises from the lower rate of reservoir thermal depletion (due to less heat extracted).

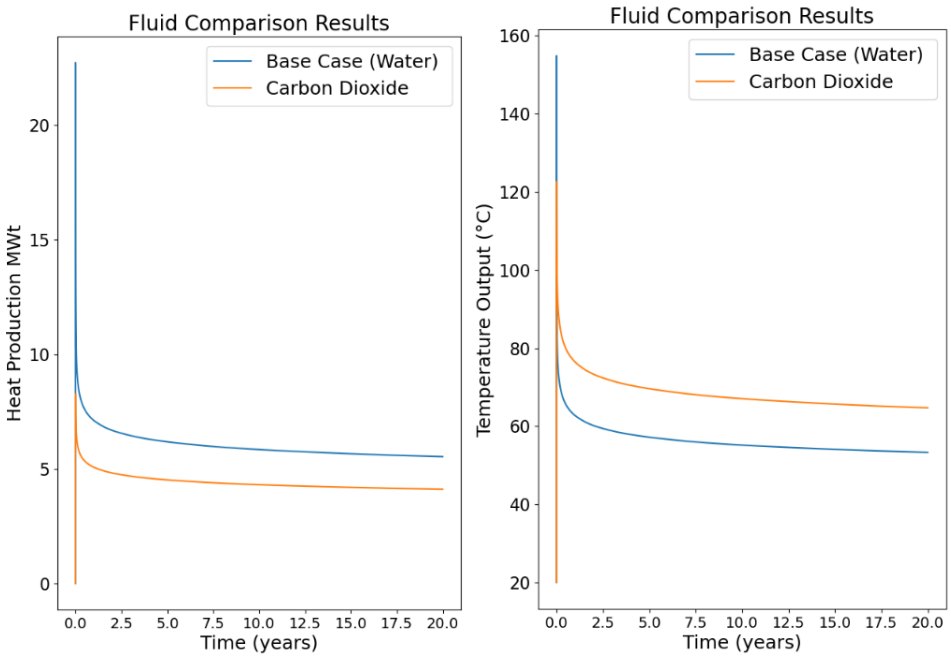

Figure 10: Heat production (MW_{th}) and temperature (°C) output over 20 years for CO_2 and water.

3.4 Optimal Well Design

An optimal well design scenario for both heat production and outlet temperature maximization has been developed based on the observed parameters and their effects over a 20-year lifetime. This scenario includes a production and injection well that was 6.1 km deep with a 0.108-m radius. Connecting the two wells are 10 laterals with radii of 0.108 m, 50-m spacing between each of the ten laterals in the X-dimension, and a well spacing of 1,000 m in the Y-dimension (Figure 11). To maximize heat production, the injection temperature is held constant at 20°C, with a constant injection rate of 60 kg/s, and flow divided evenly over the 10 laterals. The reservoir rock is granite, with an average thermal conductivity of 3.1 W m^{-1} K^{-1}, average heat capacity of 1,185 J kg^{-1} K^{-1}, and a density of 2,540 kg m^{-3}. A constant ground surface temperature was selected at 20°C and the geothermal gradient through the subsurface was 60°C/km. Water was the utilized working fluid. The pressure at the injection wellhead was 100 bar. Outputs of the system are summarized in Table 4. The trends in heat production and outlet temperature over time are summarized and compared to the base case in Figure 12. It is important to highlight that this is the performance-optimized design. The techno-economic feasibility of drilling and developing such a system is discussed in Section 4.

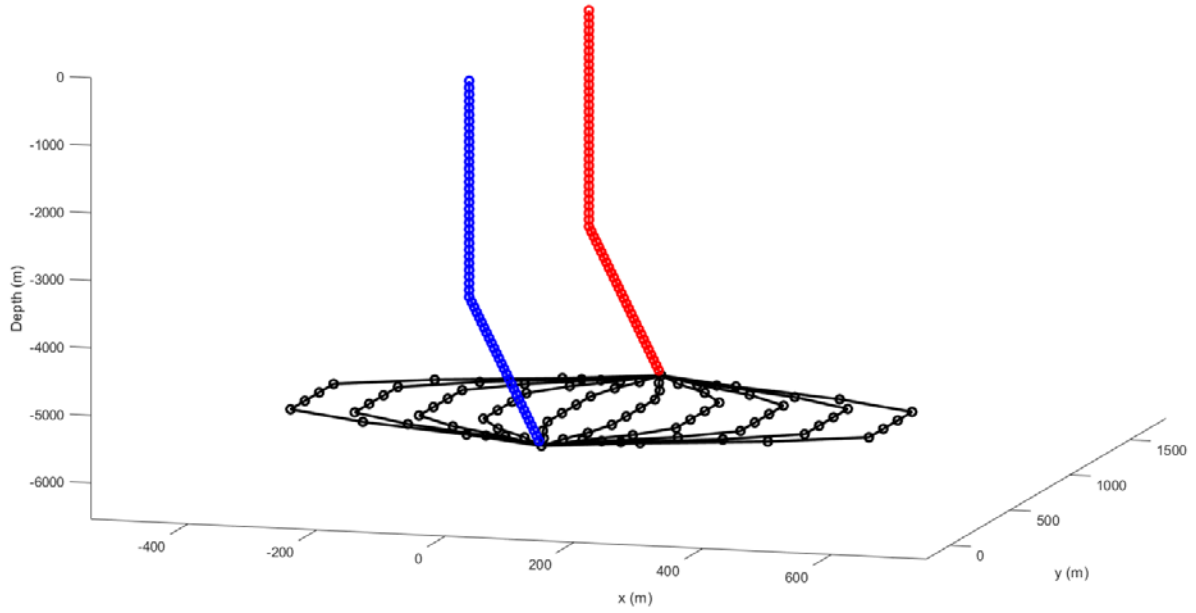

Figure 11: Optimized geometry schematic developed from observed outputs of prior scenarios.

Table 4: Inputs and outputs parameters for the optimized heat production case scenario for water after a 20-year simulation.

Parameter	Unit	Value
Input		
Injection Rate	kg/s	60
Injection Temperature	°C	20
Geothermal Gradient	°C/km	60
Number of laterals		10
Lateral Length	m	1000
Well Spacing	m	50
Rock Type		Granite
Output		
Average outlet temperature	°C	95.7
Average heat production	MW_{th}	19
Final temperature	°C	88.8

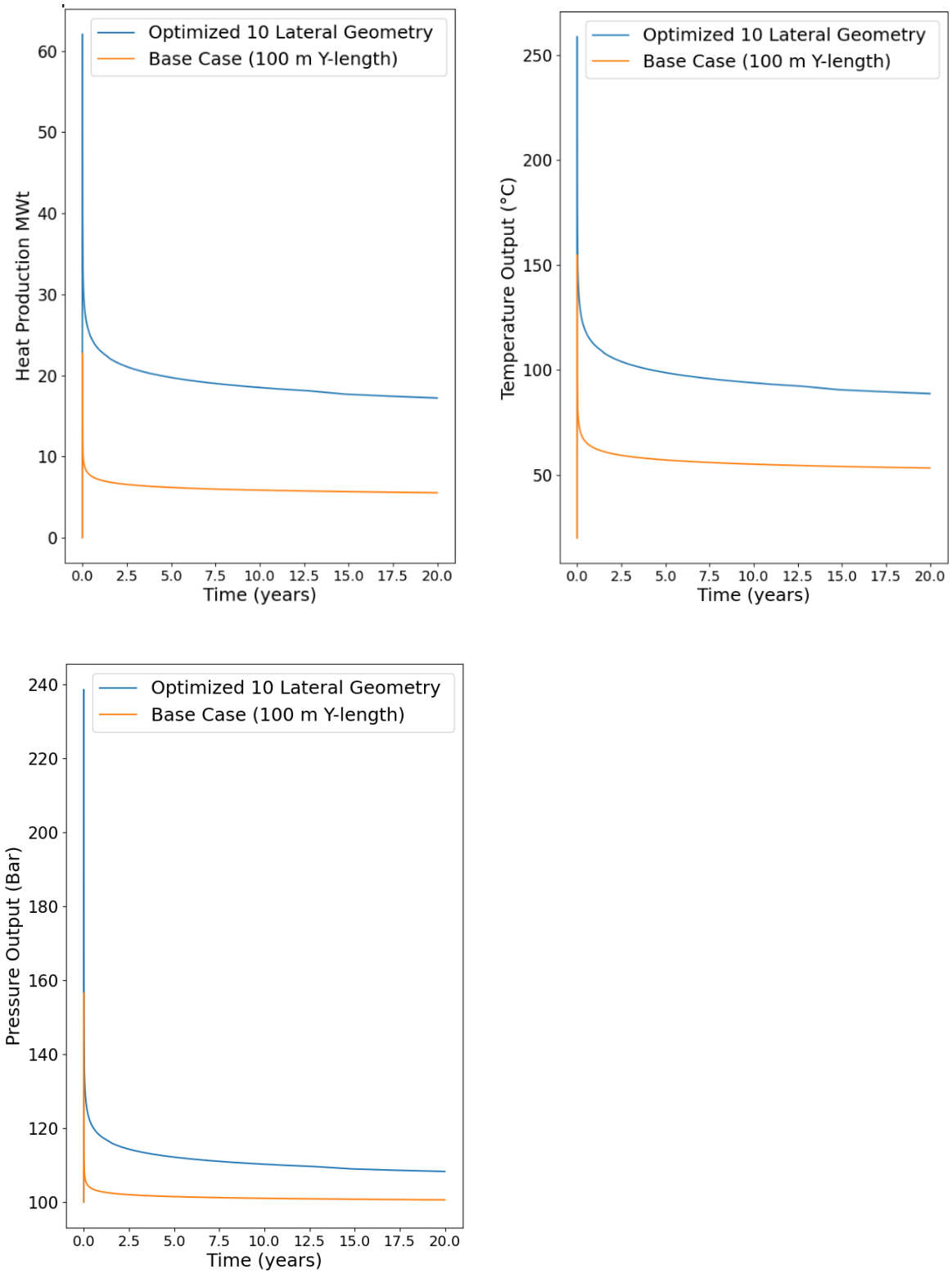

Figure 12. Optimized versus base case heat production, temperature output, and outlet pressure over 20 years for maximized heat production.

4. Techno-Economic Assessment

We have developed a simplified techno-economic assessment (TEA) model to estimate the lifecycle costs of the performance-optimized U-loop system. The TEA is a top-down Excel-based model that estimates the capital cost, operation and maintenance (O&M) costs, and the levelized costs of energy (electricity or heat). The input assumptions used in the model are listed in Table 5. These assumptions cover unit costs for the surface plant (for electricity generation only) installation and directional drilling. The model does not include the cost of project financing and does not account for tax credits or other incentives that can improve project economics.

Table 5: Input assumptions for parameters in the TEA model.

Parameters	Baseline Value	Parameter Variability	References
Power conversion factor, %	12%	10-15%	Beckers and Johnston (2022)
Plant availability, %	95%	-	Beckers and Johnston (2022)
Lateral cost per meter, $/m	600	400-800	Beckers and Johnston (2022)
Vertical cost per well, $	7,500,000	-	Beckers and Johnston (2022)
Power plant installation cost, $/kW	2,500	-	Beckers and Johnston (2022)
Heat exchanger cost, $	1,250,000	-	Beckers and Johnston (2022)
O&M as percent of capital cost, %	1.5% (electricity) 1% (heat)	-	Beckers and Johnston (2022)
Plant lifetime, yr.	20	-	
Discount rate, %	7%	5-9%	Beckers and Johnston (2022)

To determine the performance- and cost-optimized system, we executed the TEA model using the baseline input assumptions (Column 2 in Table 5) and the optimal values of the U-loop design parameters identified in Section 3 and listed in Table 4. The resulting levelized cost of electricity (LCOE) and levelized cost of heat (LCOH) were \$136/MWh$_e$ and \$1.53/GJ, respectively. Additionally, to account for uncertainty in the TEA parameters we considered six other optimal cases with variability in power plant conversion factor, lateral drilling cost, and discount rate. The results are shown in Table 6. These show that the LCOE can be further improved with higher efficiency power conversion systems while the LCOH benefits from lower discount rates. Drilling costs are important for both electricity and heating use cases with a larger degree of impact in the heating case.

Table 6: Output from the TEA modeling for both electricity and heating use cases for the optimal closed-loop design.

Parameter	Unit	Optimal I	Optimal II	Optimal III	Optimal IV	Optimal V	Optimal VI	Optimal VII
Power Conversion Factor	%	12	10	15	12	12	12	12
Lateral Cost per m	$/m	600	600	600	400	800	600	600
Discount Rate	%	7	7	7	7	7	5	9
Plant power output (electric)	kW_e	2,166	1,805	2,708	2,166	2,166	2,166	2,166
Plant power output (heat)	kW_{th}	18,050	18,050	18,050	18,050	18,050	18,050	18,050
Capital cost (electric)	$/$kW_e$	13,164.82	15,297.78	11,031.86	13,072.48	13,257.16	13,164.82	13,164.82
Annual O&M cost (electric)	$/$kW_e$-yr	197.47	229.47	165.48	196.09	198.86	197.47	197.47
Capital cost (heat)	$/$kW_{th}$	1,349.03	1,349.03	1,349.03	1,337.95	1,360.11	1,849.63	1,349.03
Annual O&M cost (heat)	$/$kW_{th}$-yr	13.49	13.49	13.49	13.38	13.60	18.50	13.49
20-yr LCOE	$/$MWh_e$	135.69	156.58	114.80	125.74	145.64	115.99	156.79
20-yr LCOH	$/GJ	1.53	1.53	1.53	1.39	1.66	1.30	1.77

4. Conclusion

In this paper, we have implemented the SBT model to investigate the thermal profiles and well production performance of a U-loop well drilled into the Wattenberg area of the Denver-Julesburg Basin. A scenario-based assessment of the effect of input variables, categories as the well geometry, boundary conditions, and rock and fluid properties, on heat transfer and well production performance was implemented. This model-enabled assessment revealed that a U-loop design characterized by an injection to production well spacing of 1,000 m with ten 50-m-spaced laterals that traverse a conductive subsurface system with a temperature gradient of 60°C/km maximizes thermal energy production. Specifically, injecting 20°C-water at a rate of 60 kg/s through the optimized U-loop, an average heat production of 19 MW_{th} (i.e., 2.2 MW_e net plant output) was achieved, resulting in an LCOE and LCOH of \$136/MWh_e and \$1.53/GJ, respectively.

Acknowledgement

This work was authored by the National Renewable Energy Laboratory, operated by Alliance for Sustainable Energy, LLC, for the U.S. Department of Energy (DOE) under Contract No. DE-AC36-08GO28308. Funding was provided by the U.S. Department of Energy Office of Energy Efficiency and Renewable Energy (EERE) Geothermal Technologies Office (GTO). The views expressed in the article do not necessarily represent the views of the DOE or the U.S. Government.

REFERENCES

Abbott, D. M., Jr., & Noe, D. C. (2004). The consequences of living with geology: A model field trip for the general public (second edition). In E. P. Nelson & E. A. Erslev (Eds.), *Field Trips in the Southern Rocky Mountains, USA* (Vol. 5, p. 0). Geological Society of America. https://doi.org/10.1130/0-8137-0005-1.185

Barrett, J. K., & Pearl, R. H. (1978). *Bulletin 39—An Appraisal of Colorado's Geothermal Resources* [Bulletin]. Colorado Geological Survey, Department of Natural Resources. https://coloradogeologicalsurvey.org/publications/geothermal-resources-colorado-2/

Beckers, K. F., & Johnston, H. E. (2022). *Techno-Economic Performance of Eavor Loop 2.0* (NREL/CP-5700-81887). Stanford, CA: Stanford University. https://www.osti.gov/biblio/1972816

Beckers, K. F., Koch, D. L., & Tester, J. W. (2015). Slender-body theory for transient heat conduction: Theoretical basis, numerical implementation and case studies. *Proceedings of the Royal Society A: Mathematical, Physical and Engineering Sciences*, *471*(2184), 20150494. https://doi.org/10.1098/rspa.2015.0494

Beckers, K. F., Rangel-Jurado, N., Chandrasekar, H., Hawkins, A. J., Fulton, P. M., & Tester, J. W. (2022). Techno-Economic Performance of Closed-Loop Geothermal Systems for Heat Production and Electricity Generation. *Geothermics*, *100*, 102318. https://doi.org/10.1016/j.geothermics.2021.102318

Crowell, A. M., Ochsner, A. T., & Gosnold, W. (2012). Correcting Bottom-Hole Temperatures in the Denver Basin: Colorado and Nebraska. *GRC Transactions*, *36*, 201–206.

Curtis, B. F. (1988). Sedimentary rocks of the Denver basin. In L. L. Sloss (Ed.), *Sedimentary Cover—North American Craton: U.S.: Vol. D-2* (pp. 182–196). Geological Society of America. https://doi.org/10.1130/DNAG-GNA-D2

Davalos-Elizondo, E., Kolker, A., Taverna, N., & Holt, E. (2023). *Assessing Low-Temperature Geothermal Play Types: Relevant Data and Play Fairway Analysis Methods* (NREL/TP-5700-87259). National Renewable Energy Laboratory (NREL), Golden, CO (United States). https://doi.org/10.2172/2001118

Eaton, M. (2023). *Causes of Geothermal Temperature Anomalies In the Denver Basin: With Application to Petroleum and Geothermal Energy*. MUTDOC Consortium - Spring 2023 Sponsor Meeting, Golden, Colorado. https://protected.mines.edu/mudtoc/wp-content/uploads/sites/18/2023/05/Eaton_Spring2023.pdf

Fox, D. B., Sutter, D., Beckers, K. F., Lukawski, M. Z., Koch, D. L., Anderson, B. J., & Tester, J. W. (2013). Sustainable heat farming: Modeling extraction and recovery in discretely fractured geothermal reservoirs. *Geothermics*, *46*, 42–54. https://doi.org/10.1016/j.geothermics.2012.09.001

Higley, D. K., & Cox, D. O. (2007). Oil and Gas Exploration and Development along the Front Range in the Denver Basin of Colorado, Nebraska, and Wyoming. In D. K. Higley (Ed.), *Petroleum Systems and Assessment of Undiscovered Oil and Gas in the Denver Basin Province, Colorado, Kansas, Nebraska, South Dakota, and Wyoming—USGS Province 39* (p. 41). U.S. Geological Survey. https://pubs.usgs.gov/dds/dds-069/dds-069-p/REPORTS/69_P_CH_2.pdf

Lacazette, A., Cumell, S. P., Matt, V. J., Cottrel, M. G., Karimi, S., Marsh, B. D., & Chmela, W. R. (2024, February 12). Using Petroleum Industry Data to Locate, Characterize, and Simulate a Hot Sedimentary Aquifer Geothermal Prospect. *Proceedings*. 49th Workshop on Geothermal Reservoir Engineering, Stanford University, Stanford, California. https://geothermal.tech/wp-content/uploads/2024/02/Lacazette-et-al-2024-Stanford-Geothermal-rev-.pdf

Moeck, I. S. (2014). Catalog of geothermal play types based on geologic controls. *Renewable and Sustainable Energy Reviews*, *37*, 867–882. https://doi.org/10.1016/j.rser.2014.05.032

Nelson, P. H., & Santus, S. L. (2011). Gas, oil, and water production from Wattenberg Field in the Denver Basin, Colorado. In *Open-File Report* (2011–1175). U.S. Geological Survey. https://doi.org/10.3133/ofr20111175

Porro, C., Esposito, A., Augustine, C., & Roberts, B. (2012). An Estimate of the Geothermal Energy Resource in the Major Sedimentary Basins in the United States. *GRC Transactions*, *36*, 1359–1370.

Roberts, S. B. (2007). Coal in the Front Range Urban Corridor—An Overview of Coal Geology, Coal Production, and CoalBed Methane Potential in Selected Areas of the Denver Basin, Colorado, and the Potential Effects of Historical Coal Mining on Development and Land-Use Planning. In D. K. Higley (Ed.), *Petroleum Systems and Assessment of Undiscovered Oil and Gas in the Denver Basin Province, Colorado, Kansas, Nebraska, South Dakota, and Wyoming—USGS Province 39* (p. 45). U.S. Geological Survey. https://pubs.usgs.gov/dds/dds-069/dds-069-p/REPORTS/69_P_CH_3.pdf

Sims, P. K., Bankey, V., & Finn, C. A. (2001). Preliminary Precambrian basement map of Colorado – A geologic interpretation of the aeromagnetic anomaly map. In *Open-File Report* (2001–364). U.S. Geological Survey. https://doi.org/10.3133/ofr01364

Weimer, R. J. (1996). *Guide to the Petroleum Geology and Laramide Orogeny, Denver Basin and Front Range, Colorado* (Buletin 51). Colorado Geological Survey, Department of Natural Resources. https://doi.org/10.58783/cgs.b51.bsvl1261